CrossMark

Specific surface area and pore size distribution in gas shales of Raniganj Basin, India

Annapurna Boruah[1] · Abdul Rasheed[2] · Vinod Atmaram Mendhe[3] · S. Ganapathi[4,5]

Abstract
Understanding of multiscale transports of shale gas is important for shale gas exploration and exploitation. Traditional porosity determining approaches normally underrate the shale gas transport capacity as these techniques do not include adsorb gas in nanometer-sized slit pores. Silty shale, carbonaceous shale, claystone and ironstone shale unit of Barren Measures Formation was examined to understand the pore system at various scales. The pores are intergranular, intragranular, interlayer, dissolved pore and fracture pores where gas molecules are present as free state and/or adsorbed gas in the internal structure of the pores and at the edge of their structures. Here, we used the Brunauer–Emmett–Teller technique with scanning electron microscopy for considering the adsorption mechanism to understand the gas transport in micro and nano pores in shales. The adsorption parameters between organic wall and grain surface were observed to be controlled by clay mineralogy. SEM, X-ray diffraction and BET manifest significant information about role of clays, organic matter and mineral composition in development of pore network, which also governs the gas storage and transport properties. A large portion of pores in Barren Measures shales ranges between 20 and 55 nm and the pore size diameter ranges from 5.49 to 29.75 nm.

Introduction

The United States of America and Canada are producing profitable shale gas and contributing almost 20% of total natural gas produced (including both conventional and unconventional). The success of the Barnett Shale play in Texas has motivated the search for shale gas resources across the United States, Canada, Europe, Asia and Australia. The challenge in evaluation of shale gas resources is to identify the most prospective area, to appraise and develop them efficiently.

Shale is the sedimentary rock containing organic matter from which in situ methane gas is generated through biogenic (biogenic gas) and/or thermogenic (thermogenic gas) processes. The gas may be stored within the shale in three distinct phases (1) free gas in the micropores/ micro fractures; (2) adsorbed gas on the internal surface of the organic matter and clays and (3) dissolved phase. Therefore, gas from shale reservoirs can be explored through permeable sand or silt layers interbedded with the shale, through natural fractures, and/or from the rock matrix. The free and adsorption phases constitute the major existences of shale gas (Bowker 2003). The gas production is not well understood because of the adsorptive capability of shales which is basically governed by nano pore networks connected to a micrometer pore network which controls the gas flow. The specific surface areas of the shale includes clays, organic matter, etc. where clay minerals are the chief components of shale sediments. The clays are layered chained structured silicates and contain a large amount of nano pores, which are developed in interlayer and inter-cleavage surfaces to provide space for shale reservoir development. Moreover,

✉ Annapurna Boruah
   aboruah@ddn.upes.ac.in

1 Department of Petroleum Engineering and Earth Science, University of Petroleum and Energy Studies, Dehradun 248007, India

2 Gujarat Energy Research and Management Institute, Gandhinagar 382007, India

3 Central Institute of Mining and Fuel Research, Dhanbad 826015, India

4 The Maharaja Sayajirao University of Baroda, Gujarat 390002, India

5 ITM Universe, Gujarat 390002, India

مدينة الملك عبدالعزيز
KACST للعلوم والتقنية

Springer

micro fracture may develop during the process of diagenesis of montmorillonite into illite. This process offers massive pore space and effective channels for transportation of gas molecule (Zhao and He 2012). The pore structures of a clay mineral within shale may differ depending upon the degree of diagenesis and maturity of the shale. However, illite shows the strongest capacity for methane adsorption but it may decrease when it absorbs/holds water due to the preferential adsorption of water over methane (Ross and Bustin 2009). The internal structure and physicochemical properties of clays govern the nature of shales as well as adsorption capacity and gas storage mechanism within it. Understanding the storage mechanism and flow capacity within the shale rock can help in exploration and development of shale gas resources (Jarvie et al. 2007; Kang et al. 2010). Boruah and Ganapathi 2015a, b; Varma et al. 2014, 2015 studied hydrocarbon generation potential of shale samples from Raniganj Basin, India and recognized the shales as gas prospect for future gas shale exploration. Oil and Natural Gas Corporation Limited drilled pilot wells for shale gas exploration and identified the Barren Measures Formation as shale gas play. The present study is to understand the surface area, pore morphology and pore size distribution in Barren Measures shale of Raniganj Coal Field.

Sampling and analytical methods

We studied continuous cores of Barren Measures formation, studied lithologs and collected forty representative samples from four drilling wells of Raniganj Coal field, India (Fig. 1).

Forty samples of Barren Measures Formations were selected for X-Ray diffraction analysis and scanning electron microscopy to understand the lithofacies variation of the shales, while samples from each litho unit of Barren Measures Formation were identified for BET and transmission electron microscopy studies. The samples were pulverized and passed through the ASTM # 300 mesh using Fritsch Micro Pulverisette-7 machine. The powdered samples were scanned from 3° to 90° 2θ in a Rigaku X-Ray Diffractometer (Model Ultima-IV) with Ni-filtered Cu Kά radiation.

The rock samples were mounted on aluminium stub with double-sided metallic tape so that fresh broken surface was exposed. The samples were coated with Gold (Au) using a Polaron Sputter Coating Unit. The SEM photomicrographs were taken using JEOL, JSM-6460 LV Scanning Electron Microscope operating at 10–20 kV to bring out the desired features under high magnification up to 20,000X (Houben et al. 2013; Houben et al. 2016).

The Total Organic Content (TOC) was determined using LECO EC-12 carbon analyser (Hunt 1995).

The low pressure N_2 adsorption–desorption isotherm curves were being used for the physical sorption mechanism and the pore structures of the shales (Kuila et al. 2012). A Brunauer–Emmett–Teller (BET) technique was used to analyze the shale samples. The BET theory explains the physical adsorption of gas molecules on a solid surface and measurement of the specific surface area of shales (Brunauer et al. 1938). The technique signifies multilayer adsorption using non-corrosive gases (nitrogen, Ar, CO_2 etc.) as adsorbents to study the surface area and pore size distribution. It can be used to analyse fine pores of 1.7–200 nm (Ross and Bustin 2007; Chalmers et al. 2012). Here, the experiment

Fig. 1 Geological map of Raniganj Coal Field
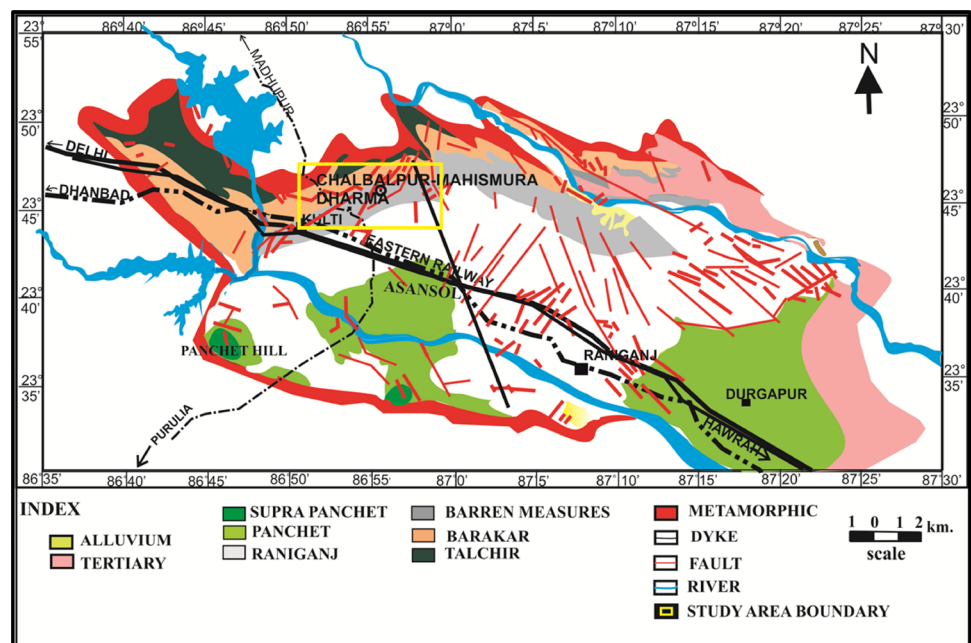
was carried out on a Micromeritics ASAP 2010™ instrument. The quantity of adsorbed gas on the solid surface was measured at discrete pressure (P) steps over the relative equilibrium pressure ($P/P0$) range of 0.28518 to 0.973288 at constant temperature. The key assumptions used for reversing the isotherm data to get micropores volume and pore size distribution (PSD) by t-plot and BJH technique, respectively, which is the thickness equation that quantifies the thickness of the adsorbed layer on the pore surface as a function of relative pressure ($P/P0$). The shape of the isotherm and its hysteresis pattern provide useful information about the physisorption mechanism. IUPAC (International Union of Pure and Applied Chemistry) classified the adsorption isotherms into six types (Type I–VI), along with desorption four-hysteresis isotherms pattern types (H1–H4). These isotherm types, especially important for unconventional gas are described here (Figs. 2, 3). The hysteresis patterns suggest about the texture, pore size distribution, pore geometry and connectivity within shales. The BET analysis evaluates the specific surface area originated in the samples by N_2 multilayer adsorption measured as a function of the rise in relative pressure.

According to IUPAC (Singh et al. 1985) classification of pores system, the pores ranges from < 2 nm size are considered as micropores; 2–50 nm considered as mesopores and > 50 nm were emphasized as macropores. They include multilayer adsorption (macropores), a combination of multilayer adsorption and capillary condensation (mesopores), and micropore filling (micropores). The distribution of pore volume can be displayed as incremental or differential distribution and cumulative curves (Chalmers et al. 2012; Kuila and Prasad 2013).

Results and discussion

Mineralogy and organic content

Quartz content ranges from 45 to 69%, which is highest in silty shale unit while other minerals in Barren Measures shale are albite (AL), andolusite (AN), barite (BT), beryl (BY), chlorite-montmorillonite(C-M), chlorotoid (CHLT), clinoclore (CL), illite (I), ilmenite (IL), kaolinite (K), leucite (L), microcline (MCR), montmorillonite (M), muscovite
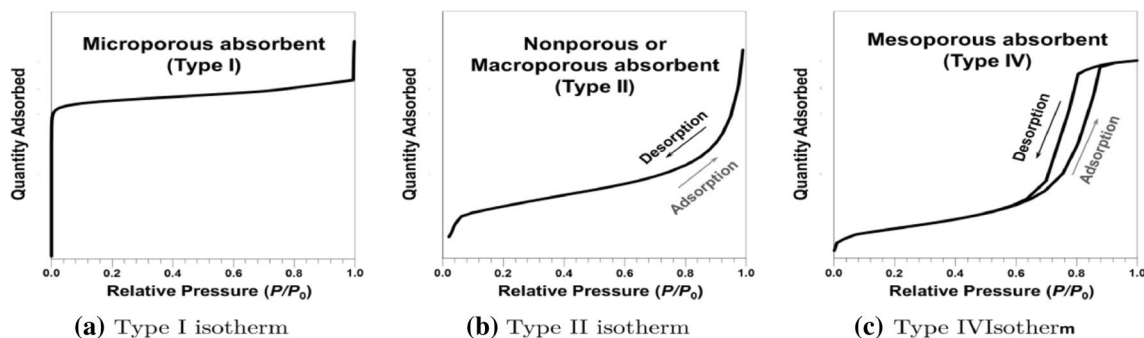

Fig. 2 Typical isotherm shape **a** microporous (Type I isotherm profile), **b** non-porous and macroporous (Type II isotherm profile) and **c** mesoporous (Type IV isotherm profile). Modified from Singh et al. (1985)
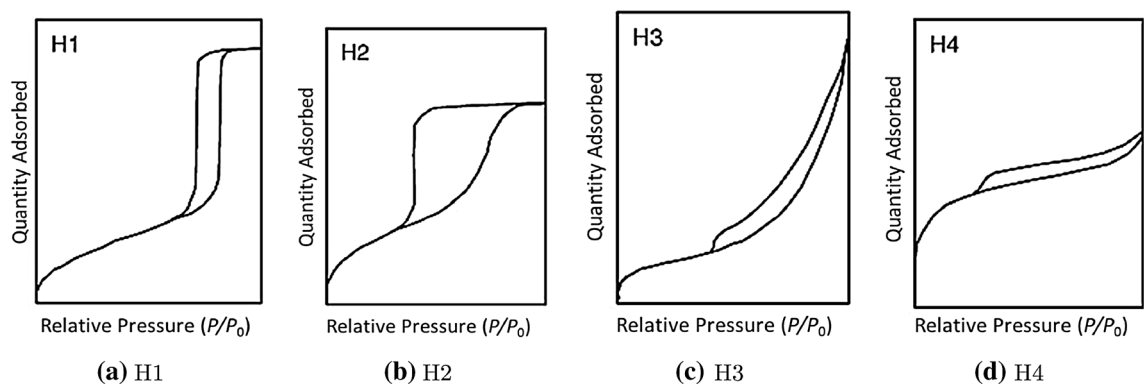

Fig. 3 The four hysteresis shapes of adsorption isotherm usually found by subcritical N_2 adsorption. Modified from Singh et al. (1985)

(M), orthoclase (O), pyirite (P), pyrolusite (PY), pyrrhotite (PYRH), and siderite (S).

The clay minerals (e.g., smectite, kaolinite, illite, chlorite, etc.) are always abundant in siliciclastictic hydrocarbon reservoirs. They are one of the indicators of sedimentation and tectonics, hydrocarbon generation and expulsion and play important role in formation and development of the shale gas reservoirs. A set of data was obtained for mineral composition analysis of samples using thin section analysis and X- ray diffraction techniques. The common clay minerals of the sediments comprised of illite (I), chlorite (CHL) and chlorite-montmorillonite (CHL/M), kaolinite (K), chloritoid (CHLT), smectite (S), montmorillonite (M) and clinochlore (CL). Clinochlore is the most abundant clay in all the samples analyzed (Table 1; Fig. 4). Clay minerals present in various compositions depending on their parent rock or provenance and depositional environments with a mean content of 26.96%, 43.21%, 20.78%, and 34.62% for carbonaceous shale, silty shale, claystone shale and iron stone shale litho units, respectively. On the other hand, total organic content of the shales varies widely for carbonaceous shale (> 11%), silty shale (7–12%), claystone shale (4–10 wt%) and iron stone (4–7 wt%) shale litho units.

Different morphotypes clays were identified by SEM images interpretation. The booklet kaolinite plates (Fig. 4g) are 1–5 μm across and up to 8 μm in length. Kaolinite forms well-developed euhedral, blocky crystals and clusters of booklet-like grains and these are partially filling the primary and secondary pore spaces. The platy kaolinite precipitated on authigenic quartz crystals. The authigenic kaolinite crystals are well developed in areas where authigenic feldspar is ill developed. XRD results also indicate the presence of kaolinite and chlorite (Fig. 4). Presence of various types of clay minerals indicates different depositional environment, climatic condition, composition of river water or intensity of diagenesis. The significant changes in clay minerals morphology and internal structure during burial and their relations with diagenetic stages, temperature, organic matter maturity, hydrocarbon formation and primary migration/expulsion govern the shale gas generation and storage potential. Within the identical depositional environment, the formation or alteration of clay minerals by diagenesis is strongly controlled by the thermal and tectonic evolution of the sedimentary basin. The Permian sediments of Barren Measures Formation were affected by several tectonic phases including global rifting at the age of Triassic. The petrographic microscopy and scanning electron microscopy results reflect that the sediments have undergone different stages of diagenesis with respect to increasing depth. The different stages include (1) grain dissolution, (2) organic matter dissolution, (3) hematite and/or illite grain coating, (4) quartz and feldspar overgrowths, (5) siderite cementation,

Table 1 Mineral composition of different shale units from Barren Measures formation (in percentage)

Litho units	AL	AN	BY	BT	CHL	CHLT	CL	I	IL	K	L	MCR	M	MUS	ORTH	P	PY	PYRH	Qtz	S	S-K
Silty shale	8.26	0.52	0.50	0	0.22	0	21.98	1.51	0.19	0.94	0	1.14	0.21	1.01	2.7	1.50	7.60	1.16	67.15	6.12	2.1
Carboneceous	3.97	0.21	0.67	0	0.27	0.26	14.57	2.83	2.49	0.06	0.67	0.67	0.91	0	0.57	1.94	1.19	40.12	1.87	1.29	
Claystone	4.53	0.82	1.90	0.82	0.77	0.82	21.40	5.95	0	5.83	0.75	1.78	0	3.63	0.00	0.97	2.44	1.72	45.23	5.37	0
Ironstone	8.26	0.518	0.5	0	0.21	0	21.98	1.51	0.19	0.943	0	1.14	0.21	1.0	0	1.5	7.6	1.16	55.71	6.124	2.1

Fig. 4 Classification of lithofacies of Barren Measures shale based on mineralogy, petrography andscanning electron microscopy. I. **Silty shale**: photomicrographs (**a**) & (**b**) illustrate sub rounded quartz grains coated with clays. II. **Carbonaceous shale**: Photomicrographs (**c**) and (**d**) indicate presence of organic matters where grains are coated with iron. III. **Claystone**: (**e**) indicates presence of clays; (**f**) booklet type of kaolinite clays. IV. **Ironstone shale**: (**g**) iron precipitation in the microfractures; (**h**) iron nodules

(6) mechanical compaction, (7) cement chemical dissolution, (8) kaolinite precipitation, (9) iron mineral precipitation, (10) illite precipitation and dissolution to create bridging effect and (11) chlorite precipitation. During different stages of diagenesis, clays are developing multi-scale and different morphologies of pores.

Pore sizes and morphology

The clay minerals are observed under SEM in crystalline form where the morphology of illite presents the fiber-like and hair filament type of structure (Fig. 5h). Kaolinite presents a book-like structure and chlorite shows petal and leaf-like structure (Fig. 5e). The pore sizes in shales can reduce because of diagenetic processes due to compaction and recrystallization of clay minerals, which reduces the overall pore space in shales. The pores between clay minerals and brittle minerals reflect the degree of pore development. The clay minerals consist of particles with anion-layered silicates and metal cations. They are part of the phyllosilicate group of minerals where either they have the "sandwich" structure with two layers of sheet silicates bonded to octahedral cations or weakly bonded cations that are located between layers and are solvated by water. Depending on deficiency in the positive or negative charge balance of mineral structures, clays can adsorb cations and anions and can retain them around its structure without affecting the basic silicate structure. These adsorbed ions are easily exchanged by other ions (Guo et al. 2013; Hao et al. 2013). The range of the cation-exchange capacities and surface areas of common clay minerals are given in the Table 2.

Adsorption analysis

The significant feature observed in many hysteresis patterns is the forced closure of desorption branch where the isotherm 'closes' at $P/P0$ relative pressures around 0.45–0.50 for N_2 isotherms (Fig. 6). This phenomenon is ascribed to a process called "Tensile Strength Effect (TSE)" (Gregg and Sing 1983). Such type of loss of the hysteresis is due to the instability of the hemispherical meniscus during capillary evaporation in pores with diameters smaller than approximately 4.0 nm. The existence of 'forced closure' in the isotherm shape may specify a significant volume of pores with diameters smaller than 4.0 nm. The adsorption curves of the studied shales of Barren Measures are of type II indicating the physical adsorption of the N_2 gas on nano pore and meso pore-to-macro pore matrix. The profiles of the isotherms signify the presence of two different type of pores (openings)

in the shale samples. The desorption curves revealed Type H2 and H3 hysteresis signifying the presence of plate-like units that give rise to ink bottle-shaped pores and slit-shaped pores, they are entitle excellent interconnected pore network cherished to the flow of gas. These type of curves are evident at characteristically three-pressure intervals, i.e., (1) an instantaneous increase for gas adsorbed at relatively low pressure (< 0.10), (2) a stable rise instead of the plateau at a middle relative pressure (0.10–0.90) and (3) sudden increase at a high relative pressure. The average surface area, pore sizes and pore volume for all analyzed samples are presented in Table 3.

The present study results specific surface area of Barren Measures shale ranges from 11.75 m^2/g to 15.11 m^2/g. The N_2 adsorption isotherm and desorption isotherms for the samples are presented in Fig. 6. The carbonaceous shale lithofacies have larger surface area 15.11 m^2/g followed by claystone (14.19 m^2/mg), silty shale (13.27 m^2/g) and ironstone facies (11.75 m^2/g). The larger surface area results from the high content of clays, organic matter and very fine grain rock matrix. The studied samples show that the adsorption desorption isotherm curves do not overlap, it results in a hysteresis loop. The type looks like type IV isotherm, caused by capillary condensation. The pore size distribution, as interpreted by BJH theory (Fig. 7) show that ironstone facies and silty shale facies have larger peak at 4 nm ($40A°$) to 10 nm ($100A°$) while other samples have limited pores below 20 nm ($200A°$) and most of the pores are in the range of 20 nm ($200A°$) to 55 nm ($550A°$). BJH adsorption reveals the pore size diameter range from 5.49 nm ($54.92A°$) to 29.75 nm ($290.75A°$). The curves indicate smooth surfaces of mesopores and the variation in the pore volume of Barren Measures is the result of microstructure heterogeneity, i.e., mineral content and volatile matters and diagenesis effects. It seems that surface area and volume decreased while the diameter of the pore increased indicating the reduction of available micro- and mesopore volumes (Chen et al. 2016).

The adsorption on minerals is controlled by surface area while different mineral have different storage capacities. Diagenesis of minerals can develop secondary pore system as well as disintegrate and reduce the grain sizes to enhance the surface areas. Clay minerals easily undergo physical deformation and chemical transformation due to its less stability and they may develop various micropores. Cationic organic molecules including certain aliphatic and aromatic amines, pyridines, and methylene blue may replace inorganic exchangeable cations present in the interlayers of clays. Polar organic molecules can replace adsorbed water on external surfaces as well as in interlayer positions. The interlayered areas of montmorillonite may enlarge to 1.7 nm in contact with water but it is at 1.0 nm for illite (Cao et al. 2015). The diameter of a methane molecule is about 0.38 nm. Therefore, the molecule can dissolved in water or
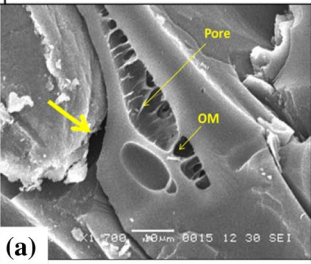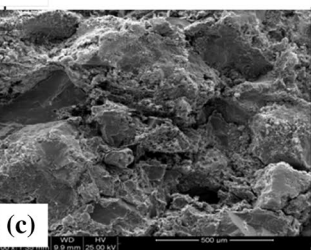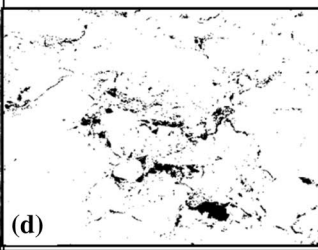
Table 2 Cation-exchange capacities and specific surface areas of clay minerals

Mineral	Cation-exchange capacity at pH 7 (milliequivalents per 100 g)	Specific surface area (m^2/g)
Kaolinite	3–15	5–40
Illite	10–40	10–100
Chlorite	10–40	10–55
Smectite	80–120	40–800
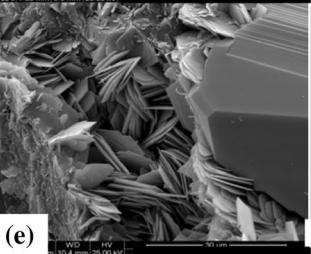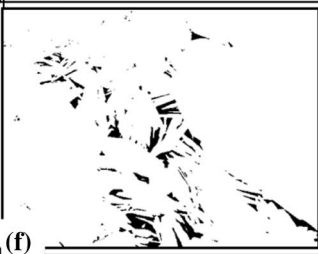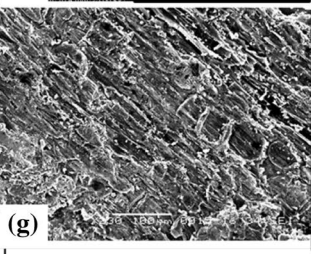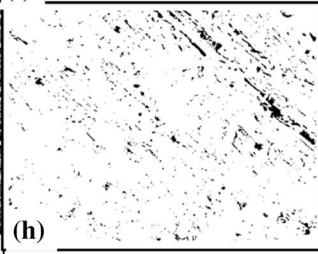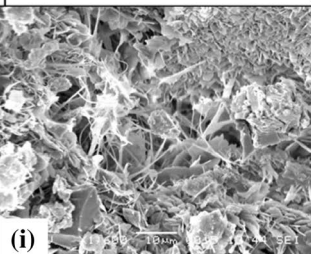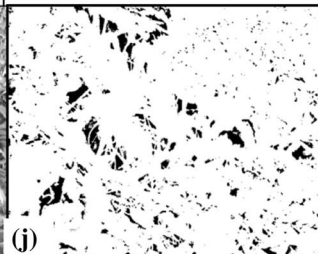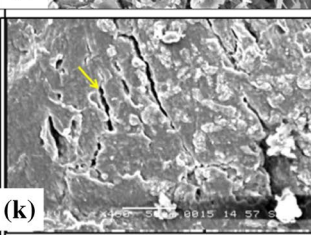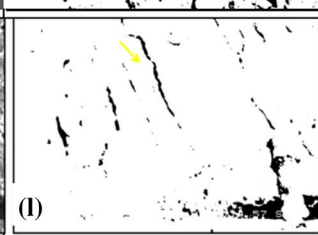
Pore description	SEM image	Pore Morphology
Dissolved pore: dissolution of organic matter; corroson by alkali and acid in clay mineral. Pores are circular and elliptical	(a)	(b)
Intergranular pore: Pore at the contact of clay mineral with other mineral	(c)	(d)
Intragranular pores: pores in chlorite. Chlorites are present in clusters, containing significant amount of pores within its structure.	(e)	(f)
Interlayered pores: pores associated with organic matter and clay surface	(g)	(h)
Pores in illite: appear as fibrous masses of fine crystals developing micro pores	(i)	(j)
Fracture porosity: Diagenesis and tectonism can develop microcracks on the clay surface	(k)	(l)

Fig. 5 Morphology and classification of pores in shales. **a** Dissolved pores, **c** intergranular pore, **e** intragranular pores, **g** interlayered pores, **i** pore in illite, **k** fracture porosity. **b, d, f, h, j** The pore distribution and network of SEM images **a, c, e, g** and **h**, respectively

Table 3 Summary results of BET analysis of shales of Barren Measures formation

Laboratory investigated parameters	(Sample 1) Claystone	(Sample 2) Carbonaceous	(Sample 3) Ironstone	(Sample 4) Silty shale
BET surface area: (m^2/g)	14.1935	15.1135	11.7592	13.2762
BJH adsorption cumulative surface area of pores (m^2/g)				
Between 17 and 3000 A diameter (m^2/g)	9.1341	15.0813	9.6205	10.4058
BJH adsorption cumulative surface area of pores				
Between 17 and 3000 A diameter (m^2/g)	15.8386	0.020716	11.488	13.4603
Volume				
Single point adsorption total pore volume of pores <744.2342 A diameter at p/po. 0.97328882(cm^3/g)	0.025267	0.02071	0.01755	0.018603
BJH adsorption cumulative pore volume of pores Between 17 and 3000 A Diameter(cm^3/g)	0.022852	0.019349	0.016346	0.017017
BJH adsorption cumulative pore volume of pores Between 17and 3000 A Diameter(cm^3/g)	0.025716	0.020707	0.17435	0.019625
Pore size				
Adsorption avg. pore diameter (4V/A by BET) A	71.2086	54.8342	59.6969	56.0497
BJH adsorption avg. pore dia (4V/A)	100.0715	60.6717	67.9649	65.4152
BJH adsorption avg. pore dia (4V/A)	64.945	54.9212	60.7055	58.3199

be stored in interlayered areas by ionic bonding. Organic molecules may also coat the surface of a clay mineral, where the surface of the constituent particles changes from hydrophilic to hydrophobic. Hence, it loses its tendency to bind water and thus, the affinity of the clays for organic matter increases, so that it can react with additional organic molecules and the surface of such clay materials can accumulate organic matters. Moreover, some of the clays can act as catalysts for reactions in which one organic constituent may change to another on the mineral's surface. In smaller nanometer-scale pores, relatively more gas molecules can be adsorbed on organic pore wall. The specific surface area of minerals play an important role in quantifying the interaction processes at the gas/liquid–solid interface. Clay minerals can provide the largest fraction of the total mineral surface area in shales because of their fine grain size as well as abundance. They are regarded as a major control of the cation exchange and of the adsorption of natural gas on the rock surface. The cation-exchange capacities and specific surface areas of clay minerals are listed in Table 2.

The pore system of Barren Measures shales can be classified into intergranular, intraparticle, dissolved pore, interlayer pore and fracture pore (Fig. 5). These pores are mostly ultra-micro-pores and micropores. However, the mesopores and macropores constitute the major parts of the pores in clay minerals. Furthermore, some micro cracks can be formed at the contact of clay minerals and organic matter or clay minerals and quartz mineral. These micro fractures can be the channels or pathways to create the pore network connecting nano/micropores and pore throats in the shale (Fig. 7).

Understanding of pore size distributions in shale is critical in assessing transport and storage behavior of the shale. The accumulation of methane in shale can be possible as the result of free and adsorbed gas in micro- and nano-size pores (Chalmer and Bustin 2008). Physical adsorption in shale can be due to the van der Waals force with the methane molecule. The chemical adsorption can be developed by the interaction of covalent bonds with the methane molecule (Zhao and He 2012). Moreover, at the early sedimentation stage, clay minerals are formed by the deposition of floccules, where well-crystallized clay minerals developed pores by direct contact from the edge to the surface, edge to edge, surface to surface. After undergoing difference phases of diagenesis like compaction and recrystallization, it loses the porosity but part of them can be preserved through mutual support by minerals (Beyene et al. 2015; Cai et al 2007, 2009; Chen et al. 2016). The studied shales show positive correlation between total clay content and pore volume and surface areas for pores with different diameters. The interrelationship among TOC, mineralogy and micropores are multifaceted due to their interactions.

Conclusion

Methane adsorption capacity is a key factor in shale gas exploration for determination of shale gas in place (GIP) while gas adsorption capacity is controlled by several geological factors like mineralogy, diagenesis, pore size and morphology, surface area, etc. Clay minerals play major role in gas adsorption on the shale rock matrix. The Barren Measures shale of Raniganj Coal Field is comprised of
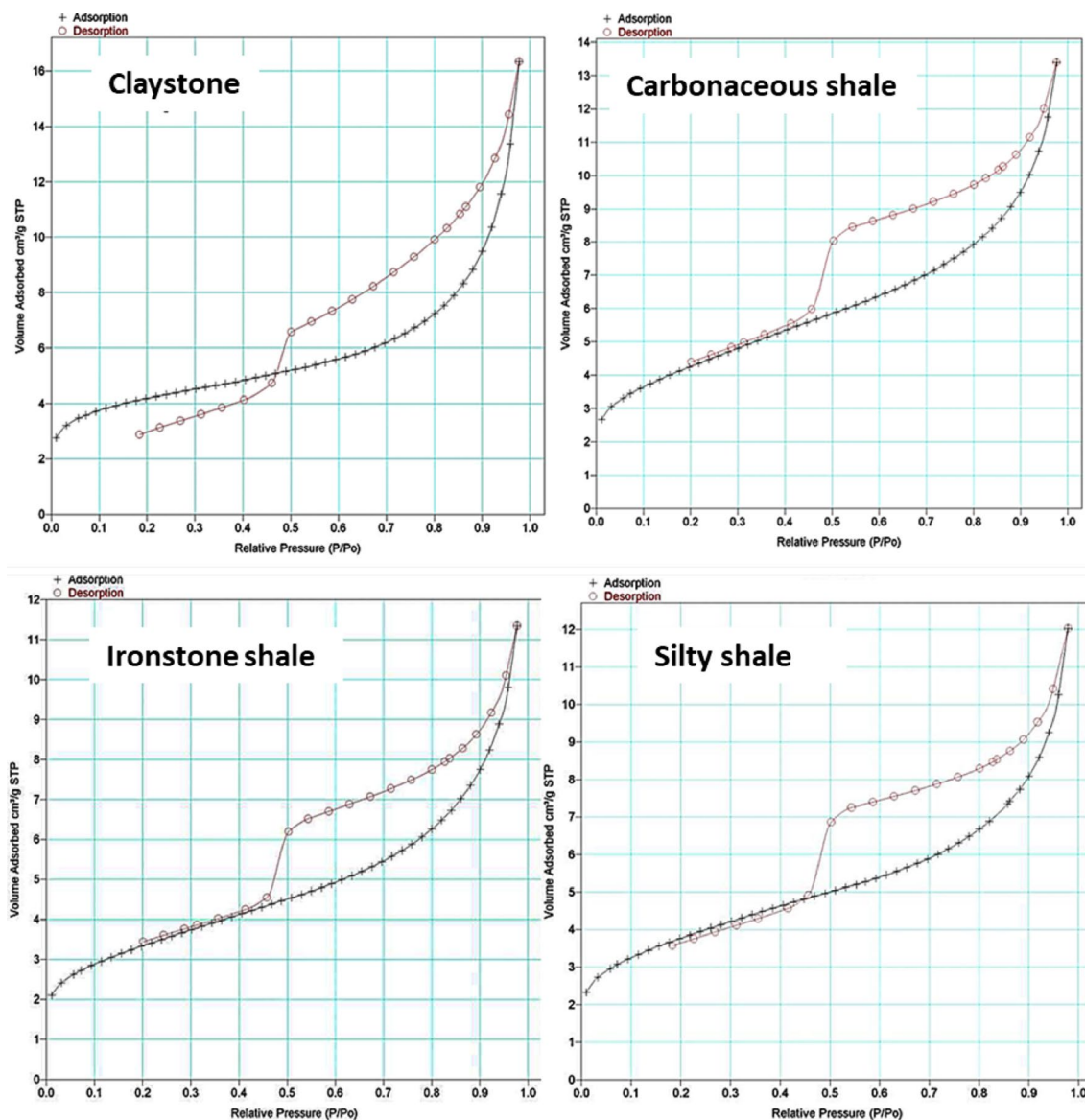
Fig. 6 N$_2$ adsorption isotherms at 77 K of a representative shale samples. B. Figure is showing the isotherm 'forced closure' in the relative pressure (P/P_0) range 0.48–0.50 due to tensile strength effect
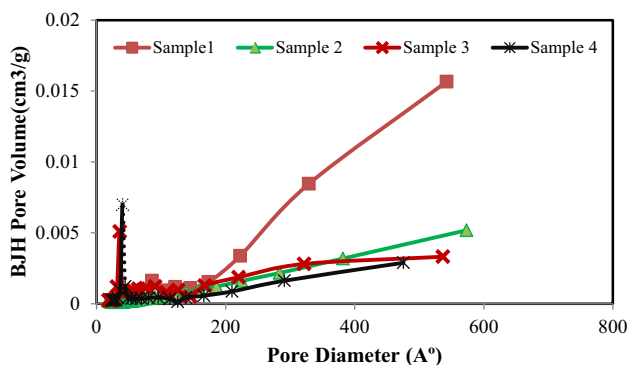

Fig. 7 BJH Pore size distributions of Permian shales

mainly illite, clinochlore, kaolinite, smectite, and chlorite clays where the clays evident great structural and morphological variations developing multiscale pores. Pores associated with shales are classified as intergranular, intragranular, interlayer, dissolved pore and fracture pores. Gas can be present in the micro-to-nano pores as free state, adsorbed gas in the internal structure of the pores and at the edge of their structures. The integrated analyses of thin section, SEM, X-Ray diffraction and BET manifest significant information about role of clays, organic matter and mineral composition in development of pore network, which also governs the gas storage and transport properties. The most of the pores are in the range of 20–55 nm

and pore size diameter ranges from 5.49 to 29.75 nm. Different units of shales in Barren Measures Formation exhibits silty shale, carbonaceous shale, claystone and ironstone where carbonaceous shales comprised of large numbers of pores followed by silty shale unit. The study infers the organic matters and clay mineral as more dominating factor for pore development and gas adsorption.

References

Beyene GH, Hellevang H, Aagaard P, Jahren J (2015) Experimental nucleation and growth of smectite and chlorite coatings on clean feldspar and quartz grain surfaces. Mar Pet Geol 68:664–674

Boruah A, Ganapathi A (2015a) Microstructure and pore system analysis of Barren Measures shale of Raniganj field, India. J Nat Gas Sci Eng 26:427–437

Boruah A, Ganapathi A (2015b) Organic richness and gas generation potential of Permian Barren Measures from Raniganj field, West Bengal, India. J Earth Syst Sci 124(5):1063–1074

Bowker KA (2003) Recent development of the Barnett shale play, Fort Worth Basin: West Texas. Geological Society Bulletin 42:1–11

Brunauer S, Emmett PH, Teller E (1938) Adsorption of gases in multimolecular layers. J Am Chem Soc 60(2):309–319

Cai J, Bao Y, Yang S, Wang X, Fang D, Xu J, Wang A (2007) Preservation ways and accumulated mechanism in muddy sediment and muddy rock. Sci China Earth Sci 37:244–253

Cai J, Lu L, Ding F, Fan F (2009) Significance of interaction between soluble organic matter and clay minerals in muddy source rocks. J Tongji Univ (Nat Sci) 37:1679–1684

Cao T, Song Z, Wang S, Xia J (2015) A comparative study of the specific surface area and pore structure of different shales and their kerogens. Sci China Earth Sci 58:139–151

Chalmers GR, Bustin RM (2008) Lower Cretaceous gas shales in Northeastern British Columbia, part I: geological controls on methane sorption capacity. Bull Can Pet Geol 56:1–21

Chalmers GR, Bustin RM, Power IM (2012) Characterization of gas shale pore systems by porosimetry, pycnometry, surface area, and field emission scanning electron microscopy/transmission electron microscopy image analyses: examples from the Barnett, Woodford, Haynesville, Marcellus, and Doig units. AAPG bull 96(6):1099–1119

Chen S, Han Y, Fu C, Zhang h, Zhu Y, Zuo Z (2016) Micro and nano-size pores of clay minerals in shale reservoirs. Sediment Geol 342:180–190

Gregg SJ, Sing KSW (1982) Adsorption, surface area and porosity, 2nd edn. Academic press, Massachusetts, pp 1–303

Guo Q, Chen X, Song H, Zheng M, Huang J, Cheng N, Gao R (2013) Evolution and models of shale porosity during burial process. Nat Gas Geosci 24:439–449

Hao F, Zou H, Lu Y (2013) Mechanisms of shale gas storage: implications for shale gas exploration in China. AAPG Bull 97:1325–1346

Houben ME, Desbois G, Urai JL (2013) Pore morphology and distribution in the shaly facies of Opalinus Clay (Mont Terri, Switzerland): insights from representative 2D BIB-SEM investigations on mm to nm scale. Appl Clay Sci 71:82–97

Houben ME, Barnhoorn LA, Trabucho-Alexandre WJ, Peach CJ (2016) Microstructures of early jurassic (Toarcian) shales of Northern Europe. Int J Coal Geol 165:76–89

Hunt MJ (1995) Petroleum geochemistry and geology. WH Freeman and Company, New York, pp 45–110

Jarvie DM, Hill RJ, Ruble TE, Pollastro RM (2007) Unconventional shale-gas systems: the Mississippian Barnett shale of north-central Texas as one model for thermogenic shale-gas assessment. AAPG Bull 91:475–499

Kang SM, Fathi E, Ambrose R, Akkutlu IY, Sigal RF (2010) CO_2 storage capacity of organic-rich shales. SPE annual technical conference and exhibition. Society of Petroleum Engineers

Kuila U, Prasad M, Derkowski A, McCarty DK (2012) Compositional controls on mud rock pore-size distribution: an example from niobrara formation. SPE 160141-PP. Presented at presentation at the SPE annual technical conference and exhibition held in San Antonio, Texas, USA, 8–10 October 2012

Kuila U, Prasad M (2013) Specific surface area and pore-size distribution in clays and shales. Geophys Prospec 61(2):341–362

Mendhe VA, Alka D, Bannerjee M, Mishra S, Mukherjee S, Mishra P (2016) Evaluation of shale gas reservoir in Barakar and barren measures formations of north and south Karanpura Coalfields, Jharkhand. J Geol Soc India 88(3):305–316

Ross DJK, Bustin RM (2007) Shale gas potential of the Lower Jurassic Gordondale Member, northeastern British Columbia, Canada. Bull Can Pet Geol 55:51–75

Ross DJK, Bustin RM (2009) The importance of shale composition and pore structure upon gas storage potential of shale gas reservoirs. Mar Pet Geol 26:916–927

Singh R (1985) Reporting physisorption data for gas/solid systems with special reference to the determination of surface area and porosity. Pure Appl Chem 57(4):603–619

Varma AK, Hazra B, Samad SK, Panda S, Mendhe VA (2014) Methane sorption dynamics and hydrocarbon generation of shale samples from West Bokaro and Raniganj basins, India. J Nat Gas Sci Eng 21:1138–1147

Varma AK, Hazra B, Chinara I, Mendhe VA, Dayal AM (2015) Assessment of organic richness and hydrocarbon generation potential of Raniganj basin shales, West Bengal, India. Mar Pet Geol 59:480–490

Zhao X, He D (2012) Clay minerals and shale gas. Xinjiang Pet Geol 33:643–648

Publisher's Note Springer Nature remains neutral with regard to jurisdictional claims in published maps and institutional affiliations.